

Received May 30, 2019, accepted June 16, 2019, date of publication June 27, 2019, date of current version July 16, 2019.

Digital Object Identifier 10.1109/ACCESS.2019.2925357

# Open Cavity Hybrid Raman-Erbium Random Fiber Laser With Common Pump

N. H. ZAINOL ABIDIN<sup>1</sup>, (Member, IEEE), M. H. ABU BAKAR<sup>1</sup>, (Senior Member, IEEE),  
Y. MUSTAPHA KAMIL<sup>1,2</sup>, (Member, IEEE), AHMAD FAUZI ABAS<sup>3</sup>,  
M. THAMER ALRESHEEDI<sup>3</sup>, AND M. A. MAHDI<sup>1</sup>, (Senior Member, IEEE)

<sup>1</sup>Wireless and Photonics Networks Research Centre, Faculty of Engineering, Universiti Putra Malaysia, Selangor 43400, Malaysia

<sup>2</sup>InLazer Dynamics Sdn Bhd, InnoHub Unit, Putra Science Park, Universiti Putra Malaysia, Selangor 43400, Malaysia

<sup>3</sup>Department of Electrical Engineering, College of Engineering, King Saud University, Riyadh 11421, Saudi Arabia

Corresponding author: M. H. Abu Bakar (mhab@ieee.org)

This work was supported by the King Saud University through the International Scientific Partnership Program ISPP under Grant ISPP#0106.

**ABSTRACT** A symmetrical 80-km open cavity erbium-integrated hybrid random distributed feedback fiber laser (HRFL) was proposed and experimentally demonstrated. A variation of pumping schemes and cavity lengths was first investigated prior to the integration of the EDF. The impact of Raman and EDF hybrid amplification was then investigated through EDF length variation. The proposed scheme used a single common pump to incite both Raman and erbium gain to produce a single peak at a 1567-nm wavelength with maximum OSNR of 62.37 dB. A maximum total output power generation of 1420 mW was achieved with high-slope efficiency of 38%. The proposed hybrid setup has shown improved performance despite using open-ended cavity sustained by only a single pump in contrast to previous more complex hybrid schemes. Prolonged chaotic regime manifesting spontaneous pulse burst was also observed before the stable regime. The simple operation with the high performance of the proposed configuration offers a great potential for long distance or remote access applications such as heavy metals sensing or even for biological hazard sensing.

**INDEX TERMS** Fiber lasers, Raman scattering, random fiber lasers, Rayleigh scattering, erbium.

## I. INTRODUCTION

Before the emergence of random laser, optical scattering was regarded as undesirable in the conventional laser scheme as it would remove photons from its respective lasing modes [1]. However, multiple scatterings in disordered gain media support laser oscillation and amplification [2], which provide a route for random lasers to operate without a classical resonator or mirrors [1]–[5]. Hence, random lasers can be constructed without a precise and costly configuration. In 2010, the concept of random distributed feedback fiber lasers (RDB-FL) employing stimulated Raman scattering (SRS) as the nonlinear gain mechanism was first reported by Turitsyn *et al.* [6], [7]. Random lasing in the optical fiber was achieved by utilizing multiple Rayleigh scattering (RS) in an inhomogeneous amplified gain medium to achieve resonance, where the intrinsic inhomogeneity of the fiber refractive index forms random virtual distributed mirrors along the cavity. The feedback from random scattering increases the path

length of the light or dwell time in the active medium [1], [3] giving rise to a larger optical gain to enable threshold generation. The continuous random feedback also enables the laser cavity length to be varied accordingly for short or large distance signal transmission.

The current situation with random fiber laser employing SRS is that it features a high threshold condition, which is due to the low gain coefficient of Raman and the weak feedback from RS. The high threshold condition of random fiber laser limits the potential applications that can be engineered, especially in circumstances where low power is the ideal. Not only that, the components within the laser is expected to be durable at very high optical power, heightening the total cost of the system. For this reason, hybrid random fiber laser was introduced [8]–[19] with the concept revolving around the fundamentals of RS-based distributed feedback but with additional characteristics from the integration of specialty fibers such as single-mode fiber (SMF) with embedded gratings [8], dispersion compensating fiber [9], [12] erbium-doped fiber (EDF) [13]–[21], ring cavity [10], and Fabry-Perot cavity [11] into the laser schemes. In comparison

The associate editor coordinating the review of this manuscript and approving it for publication was Zinan Wang.

to non-hybrid random fiber lasers, some hybrid lasers exhibit enormous reduction in the lasing thresholds accompanied with narrow linewidth [20]. The generation of higher order Raman emission was also possible at lower pump powers [9], [12]. However, prior reported hybrid schemes often used the approach of employing erbium gain [14], [15] and/or stimulated Brillouin scattering (SBS) [17], [18] instead of SRS as the gain mechanism, to lower the threshold condition. In addition to this, the systems are also feedback-assisted via half-opened [9], [11], [14], [15], [17], [19] or ring cavity [8], [11], [18] designs for fast improved results. This tendency has caused the schemes to not be fully optimized.

In this study, a hybrid random fiber laser (HRFL) is reported based on the integration of SMF and EDF. This configuration achieves random lasing through hybrid amplification from SRS effect and EDF gain, assisted by RS feedback. Our proposed hybrid random fiber laser setup yields comparable threshold conditions but with higher slope efficiency and higher output power generation relative to other hybrid configurations [9], [12], [14]–[17]. The proposed HRFL is an attractive configuration as it simply needs a single pump to sustain the laser system without requiring any physical reflectors or ring cavities, thus simplifying the laser scheme. Other Raman-erbium based random fiber laser investigations [22], [23] had also employed similar pumping scheme but were entirely different in terms of cavity design and laser generation, as [22] was dependent on a filtered seed signal for multiwavelength generation, while [23] relied on an FBG to obtain low threshold and high efficiency. Prolonged chaotic regime nonconforming of previously reported random fiber lasers is observed. Finally, the proposed scheme also confirms the behavior demonstrated by the hybrid laser reported in [12], where higher order Raman Stokes was suppressed at high pump powers.

## II. PUMPING SCHEME

To determine the best pumping scheme for the HRFL, the performance of the outward and inward pumping configuration (as shown in Fig. 1) are compared. For both cases, an open cavity is utilized with two 40 km SMF-28e fiber spools as the Raman gain medium. A 3 dB coupler is employed to equally divide the pump power from a single 1455 nm Raman pump unit (RPU) into the input ports. The outward pumping (Fig. 1(a)) is the most commonly used pumping scheme in RDB-FL [24]–[26] employing SRS. In this scheme, the pump light from RPU is injected in the middle of the cavity through a 1480/1550 nm wavelength division multiplexer (WDM). It propagates toward isolator-terminated output ports to prevent any Fresnel back reflection that can infuse undesirable Fabry-Perot effect. On the other hand, few investigations have considered inward pumping (Fig. 1(b)) for RDB-FL [27]–[29]. This structure requires pump light to be coupled into the cavity from the ends. The principle is the same for both setups, whereby pump light travels along the gain medium and is converted for the generation of SRS effect. Since the cavity length is very long, the pump light

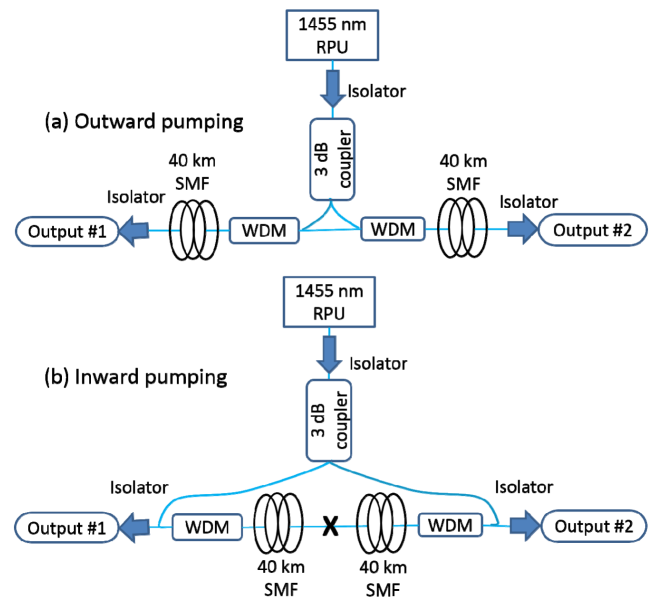


**FIGURE 1. (a) Outward pumping configuration adopted in [7] and (b) inward pumping that our proposed system adopted before the insertion of EDF (at point marked X).**

is almost fully converted into Stokes signal in the SMF-28e fiber. For this study, the total output power is taken from the summation of output #1 and output #2 as depicted in Fig. 1. However, only one side of the spectral output will be displayed as the measured results are approximately the same due to the symmetrical configuration [7].

Fig. 2(a) shows the output power evolution with respect to the total pump power. The maximum total output power obtained with outward pumping is 378 mW and 1190 mW with inward pumping at the maximum pump power (5.4 W). The slope efficiency obtained in outward pumping is 7.6 % and 29.8 % in inward pumping. In outward pumping, the equally split pump power only propagates through half the cavity length in comparison to inward pumping. Thus, a higher excess pump power unconverted to Raman Stokes is expected at the end of the cavity. Another observation that can be made is that the total power in outward pumping scheme is utilized to develop both the 1st and 2nd order Raman Stokes (see Fig. 2(b)). Ultimately, this leads to the poor power performance for the 1st order Raman Stokes in outward pumping. In the case of inward pumping, the maximum output power is three-folds higher than its counterpart. This is expected, since inward pumping scheme is almost similar to backward pumping scheme in a sense that the outputs are both located within the proximity of the pump source; the region with high gain. It is also observed that at the maximum pump power, only inward pumping achieved a stable laser, which is shown by the suppression of the stochastic modes across the Raman gain region. This shows that in developing a single wavelength non-cascaded Raman laser output, inward pumping is a more viable pumping scheme.

The inward pumping scheme is also assessed with several different cavity lengths of the same fiber to gauge the

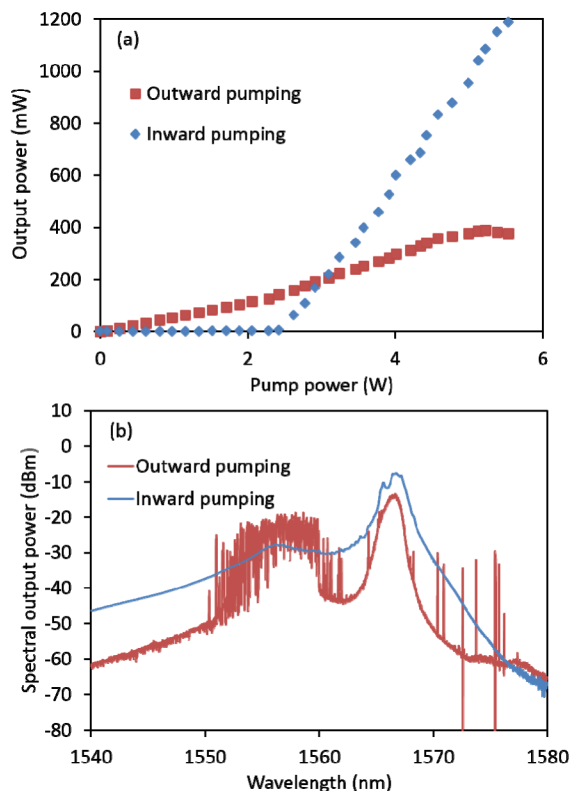


**FIGURE 2.** (a) The output power growth and (b) the spectral output of outward pumping (red and square) and inward pumping (blue and diamond) at maximum pump power (5.4 W).

possibility of shorter RDB-FL. The cavity lengths tested are 20 km, 40 km, and 60 km. The findings (not shown in this paper) presented slight improvement in the threshold with shorter cavity lengths, but a stable lasing operation is inconceivable even at the maximum pump power. A possible explanation for the stabilization of the laser with 80 km cavity length is that the additional length has granted a supplementary region where it exists to solely scatter the radiation via Rayleigh scattering. In this supplementary region Raman nonlinear effect is no longer prevalent from pump depletion; hence it does not contribute to the amplification of the radiation. However, it strengthens the resultant resonant curve which results in bandwidth reduction size and stabilization of the laser. A similar concept was also claimed in [14]. Conclusively, 80 km cavity length is maintained for the development of a stable single-peak wavelength HRFL. For later comparison purposes, the setup in Fig. 1(b) will be referred to as ‘without EDF’ or non-hybrid setup.

### III. PROPOSED EXPERIMENTAL SETUP

The experimental setup for the proposed HRFL is shown in Fig. 3. The 1455 nm RPU is launched bidirectionally through a 3 dB coupler for equal power distribution to the 1480/1550 nm WDM and into the 80 km SMF-28e. A RightWave LSL EDF (labeled as EDF) with maximum peak absorption coefficient of 16.8 dB/m at 1530 nm [13]

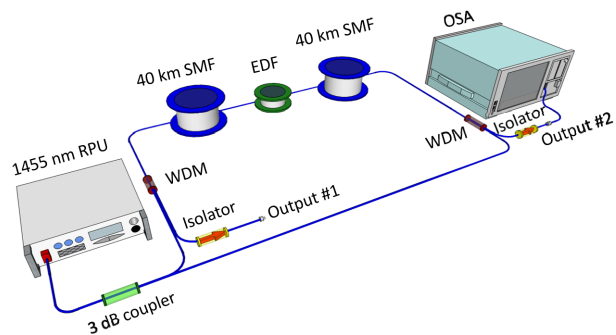


**FIGURE 3.** The proposed experimental HRFL setup.

is inserted at the center of the cavity to form the hybrid configuration. The EDF length in the setup is also varied from 10 m to 40 m with 10 m increments. Since the HRFL system also has a symmetrical structure, only a single end of the system will be measured for spectral output but the total output power will be a summation of the two output ends (output #1 and output #2) as previously done with the non-hybrid configurations. Acquisition of the generated signal is performed using an optical spectrum analyzer (OSA) with resolution of 0.01 nm and an optical power. The radio frequency (RF) spectrum and temporal mode of the signal are measured using an electrical spectrum analyzer (ESA).

The operation of the HRFL is based on the combined amplification of Raman and EDF gain as well as the resonance of Rayleigh scattering in the long length SMF. The 1455 nm Raman pump that was launched into the SMF-28e fiber instigated SRS effect with sufficiently high intensity pump power. The SRS effect shifted the 1455 nm pump radiation by about 100 nm (corresponding to 13.2 THz downshift in the silica fiber), yielding Raman Stokes in the C-band region with peak centered around 1555-1565 nm. Residual pump power that had not been converted by the Raman effect then excited the EDF. The Raman Stokes wave became the incident signal to the EDF and triggered stimulated emission. As the generated radiation propagated through the fiber, it was randomly backscattered by RS. The scattering formed random virtual distributed mirrors along the cavity which helped support oscillation essential for initiation of random lasing. As the pump power was increased, intracavity losses were overcome by the increasing gain and the threshold condition was achieved.

### IV. RESULTS AND DISCUSSION

Fig. 4(a) shows the output power development with varying pump power. The HRFL has lower near-threshold condition by a factor of 10 compared to the non-hybrid setup. However, due to the ASE noise contribution from the EDF, it is difficult to determine the exact pump power at which the threshold condition begins. This is because, the graph of generated output powers in Fig. 4(a) does not display the sharp curve associated with lasing action. Hence, the near-threshold condition

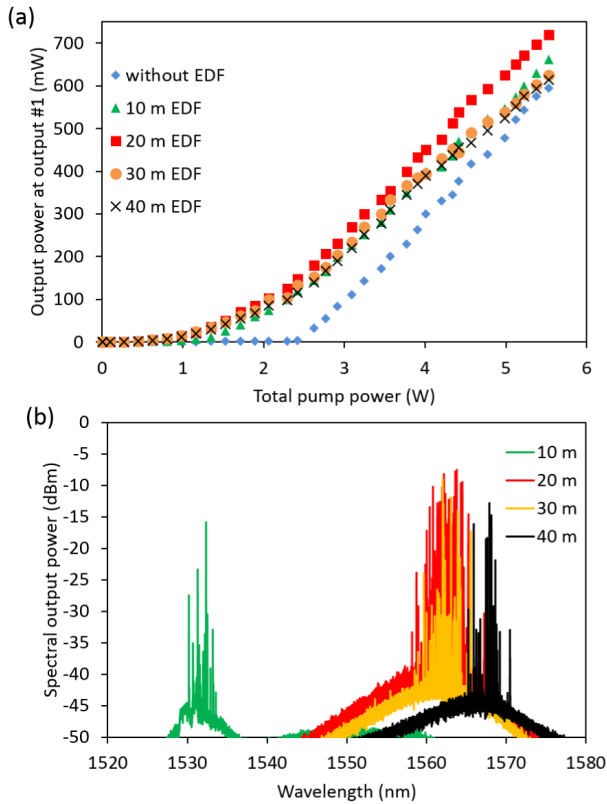


**FIGURE 4.** (a) Output power at one side with total pump power variation and (b) ASE spectrum at near-threshold condition with respect to EDF length.

of the HRFL is approximated by observing the initiation of random peaks in the spectral output (Fig. 4(b)), which is similar to the spectral behavior of conventional RDB-FL at the same condition (Fig. 2(b)). The configuration with 20 m EDF has the highest total output power and lowest near-threshold value; 1440 mW and 263 mW, respectively. The best slope efficiency is achieved by 20 m EDF with a calculated value of 38%. Comparing the HRFL to the earlier investigation on non-hybrid setup, the hybrid system reaches the near-threshold condition at lower pump power and achieves higher maximum output power, signifying the crucial role of EDF in the HRFL.

Next, the spectral output growth with increasing pump power is observed. Fig. 5 exhibits the spectrum of HRFL with 10 m EDF. The spectral development can be divided into 3 regions as depicted in Fig. 5(b); the region before the initiation of the 2nd order Raman Stokes wave (R1); the region during the growth of 2nd order Raman Stokes (R2), and lastly the region where the laser finally achieves stable stationary output with 2nd order Raman Stokes wave suppression (R3).

At 0.26 W total pump power, the low pump power is sufficient to provide inversion in the short EDF length but is incapable of instigating Raman gain, which explains the lack of Raman component in the spectrum. As the pump power increases, the 1530 nm peak starts to grow with potential lasing peaks observed. At 0.97 W, the ASE gain at 1555 nm

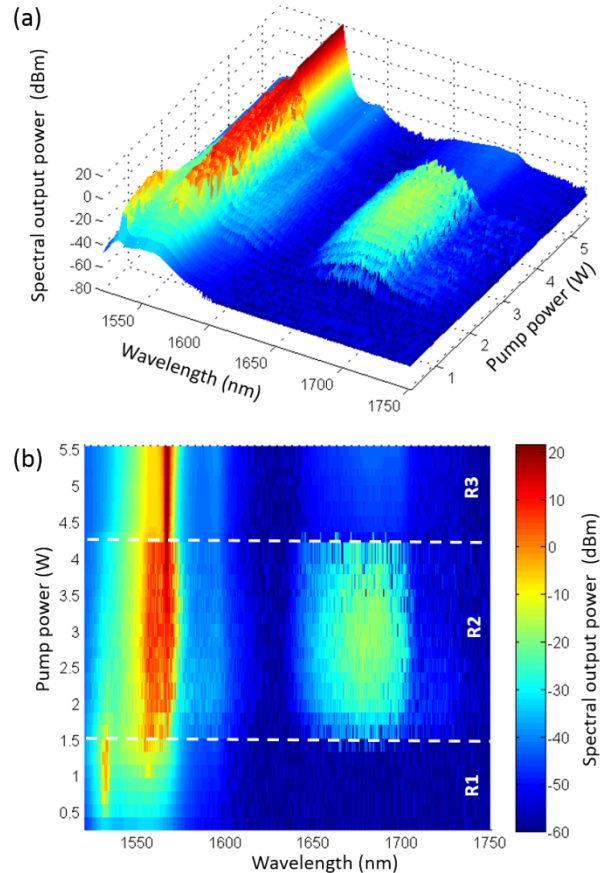


**FIGURE 5.** (a) 3D view and (b) top view of the spectral output from HRFL with 10 m EDF at various pump power.

wavelength becomes higher with stochastic peaks appearing on top of it. This marks the onset of hybrid EDF and Raman gain coexisting together. However, at 1.15 W the modes at the 1530 nm gain peak suppresses the stochastic peaks near 1555 nm region. At this point, the EDF gain has higher net amplification compared to Raman gain due to the low pump power used. With increasing pump power, the dominant gain wavelength continues to shift to longer wavelength. This is due to the Raman effect that grows with pump power, shifting the net gain profile towards the dominant Raman gain wavelength at the 1555-1565 nm region.

At 1.34 W pump power, the HRFL has entered R2 where stochastic components are instigated across the spectral profile, and elevated emission is observed around 1690 nm correlating to the 2nd order Raman Stokes shift. The 2nd order Raman Stokes stochastic emission increases from 1.34 W to 2.05 W pump power, and maintains its shape up to 4.01 W pump power. This suggests that the total power generated near the 1st order region is sufficient to drive the 2nd order Raman Stokes generation. At 4.20 W, the overlap between the EDF gain and gain from SRS has amplified the 2nd peak of the initial Raman gain region (1565 nm). At 4.34 W, a smooth stable laser at 1567 nm is observed with complete attenuation of 2nd order Raman Stokes (R3). The suppression



of the 2nd order Raman Stokes emission at higher pump powers was also observed in [12], which is attributed to the complex nonlinear effects broadening the 1st order Stokes signal. Thus, the threshold generation of the 2nd order Stokes is raised and leads to the diminished emission in the 2nd order Stokes region.

Subsequently, extending the EDF length in the HRFL to 20 m, 30 m, and 40 m, show spectral growths with similar transitions with respect to pump power. The total pump power at which the initiation (1.34 W), suppression of the 2nd order Raman Stokes (4.01 W), and the formation of stable hybrid lasing (4.20 W) occur at approximately the same pump power for 20, 30, and 40 m EDF. Fig. 6 shows the HRFL with 30 m EDF to demonstrate the transitions. With increasing pump power, it can be observed that the peak shifts to longer wavelength, similar to what has been observed in 10 m EDF HRFL. Hence, the gain peak shifts from 1563 nm to 1567 nm (see Fig. 6(b)). As with 10 m EDF, the random cavity modes of 20 m, 30 m, and 40 m EDF are also influenced by resonant wavelength of higher net gain, eventually converging to a stable 1567 nm lasing.

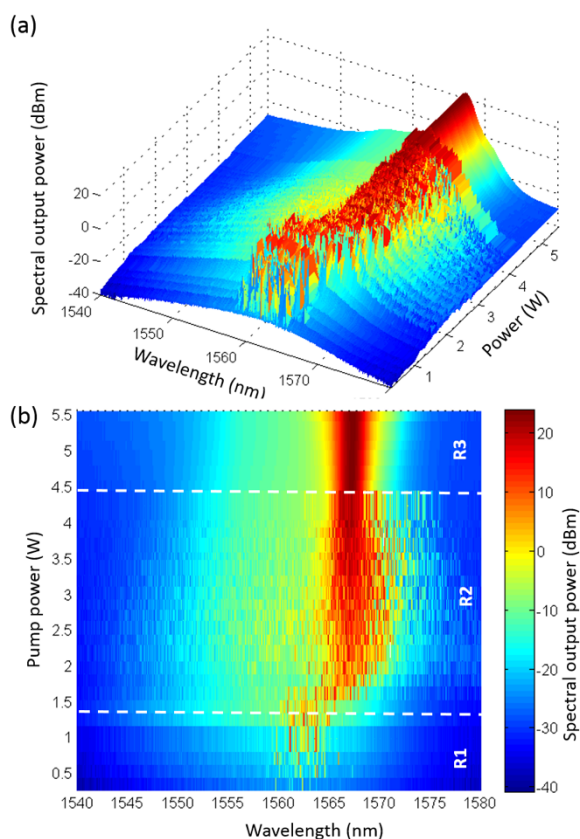


FIGURE 6. (a) 3D view and (b) top view of the spectral output from HRFL with 30 m EDF at various pump power.

The observation on the overall spectral behavior has highlighted that the insertion of EDF causes the system to be prone to multiwavelength generation. This is manifested by the escalated amount of the stochastic components and its

extensive distribution across the spectral profile wavelength compared to prior EDF integration. The homogenous gain broadening of EDF supports the abundant random wavelength components, prolonging the stochastic emission over a wider range of pump power. Due to the lack of a seed wavelength or reflectors, a biased net gain via heightening of the Raman gain is required to trigger the transition from chaotic to stable emission.

Interestingly, increasing the EDF length results in the reduction of the 1555 nm gain peak and the elevation of the 1595 nm gain peak as exhibited in Fig. 7(a). With 40 m EDF, the 1555 nm gain peak is completely flattened while the 1595 nm gain peak is the highest compared to the other EDF lengths. This effect is caused by the reabsorption of the C-band emission in the unpumped section of the EDF, which results in the shifting of the net gain profile towards longer wavelength. The amplification in the longer wavelength is heightened with the extension in EDF length, as exhibited by the growing 1595 nm peak. This also causes the initiation of stochastic components to form at a longer wavelength with the increase in EDF length.

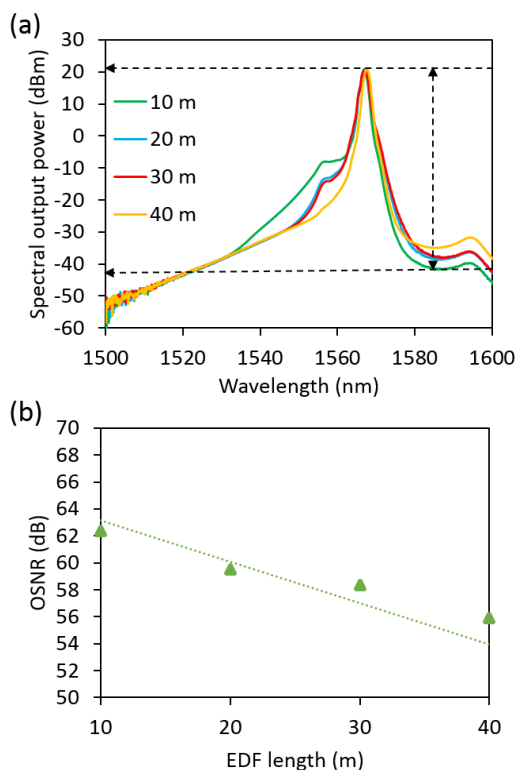
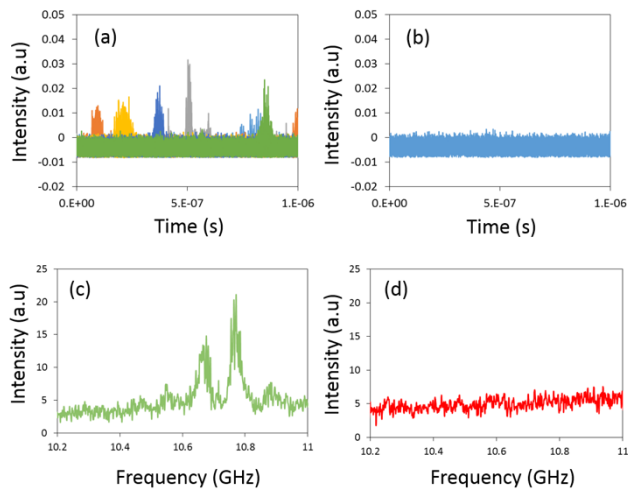


FIGURE 7. (a) Spectral profile of HRFL at maximum pump power and (b) OSNR at 1565 nm peak with EDF length variation.

The optical to signal noise ratio (OSNR) measurements with respect to EDF length is shown in Fig. 7(b). The OSNR of the HRFL is measured using OSA starting from the 1567 nm peak to the noise floor at 1586 nm as exhibited in Fig. 7(a). 1586 nm is chosen as the reference noise wavelength as it is the intermediate region connecting both

1565 nm and 1595 nm peaks. The trend shows that the OSNR deteriorates with longer EDF length. The maximum OSNR achieved is by 10 m EDF at 62.37 dB while the lowest is by 40 m EDF at 55.89 dB. The extension of the EDF has influenced the emission to absorption coefficient to be higher near the 1595 nm region, subsequently raising the noise level at 1586 nm. Despite the 1565 nm peak varying no more than 1 dB, a large OSNR deterioration occurs from 10 m to 40 m EDF from the raised noise level.

The radio-frequency (RF) spectrum and temporal performance of the HRFL with 30 m EDF are measured by using a 16 GHz electrical spectrum analyzer. Figure 8(a) shows the temporal behavior during the chaotic regime and Figure 8(b) at the stable regime. Meanwhile, Figure 8(c) and (d) shows the RF output during the chaotic regime and stable regime, respectively. When the pump power is maintained at 0.10 W, the optical spectrum is comprised solely of ASE gain from the EDF, hence the temporal and RF domain show no activity. Once the pump power is increased to 0.20-0.26 W where the near-threshold condition occurred, high intensity random pulsing in the temporal domain are observed (Fig. 8(a)) with peaks at 10-11 GHz corresponding to Stokes shift of SBS in the RF domain (Fig. 8(c)). The high intensity random pulses occur in split second, and erratically.



**FIGURE 8.** Temporal behavior in (a) the chaotic regime and (b) stable regime. Radio-frequency output in the (c) chaotic regime and (d) stable regime.

The pairing of the RF and time domain behavior is named as the chaotic regime in this paper. The Raman/EDF amplified cavity modes that were able to overcome intracavity losses and stimulate SBS caused a rapid and strong increment of the Q-value of the cavity, which produced random high intensity pulsing [30]. As the nature of these modes were volatile, the pulses appeared and vanished abruptly. Although the prolonged stochastic pulse bursts regime seems similar to the pulse bursts exhibited in [31], the pulse train lacked coherency. The chaotic regime lasted from 0.20-4.20 W pump power. The prolonged chaotic regime in contrast to

SMF-based RDB-FL in [6] is due to the chaotic emission from the EDF [16]. The noisy and random spatially distributed EDF spontaneous emission is a good candidate to initiate SBS, especially after its linewidth is narrowed by Rayleigh backscattering [30], [32]. Increasing the pump power to 4.20 W and above, the fiber laser enters the stable regime where the SBS RF peaks receded entirely (Fig. 8(b)), manifesting stable CW in the temporal domain (Fig. 8(d)). The repression of the SBS peaks in RF domain is explained in [33] as originating from the nonlinear spectral broadening of the stochastic spikes due to cross phase modulation and four wave mixing.

From the analyses, the HRFL exhibits substantially higher power generation and efficiency as well as lower threshold compared to non-hybrid system. Random fiber lasers which employed EDF as the sole gain medium achieved even lower threshold but with slope efficiencies of only 14% despite using reflectors [14], [15]. Raman-based random fiber laser investigation in [34], [35] was able to achieve high efficiency up to 75-85%. However, our work demonstrated better OSNR than in [34], [35] due to the suppression of higher order Raman Stokes. This shows that employing both SRS and erbium gain is key to better performance balance in random fiber laser schemes.

Comparing the proposed scheme to previously reported hybrid Raman-EDF scheme with same pumping design but is assisted by FBG and circulators on both extremes of the cavity [28] the proposed scheme has comparable OSNR (60 dB), but higher near-threshold condition by 200 mW, which is expected due to the absence of physical reflector. An open-ended cavity hybrid system reported in [16], employed a mix of inward pumping and outward pumping using multiple pumps to separately power the EDF and SRS. Despite the costlier configuration, the peak power and OSNR in [16] is 10 dB lower compared to the proposed hybrid scheme.

## V. CONCLUSION

A hybrid Raman-erbium random fiber laser with low threshold condition and high OSNR is demonstrated. The proposed open-ended hybrid scheme was sustained only by a single common pump source and achieve good power performance without auxiliary feedback assistance from other components. The hybrid system's stable yet simple operation may find applications that require remote access such as heavy metals sensing or even for biological hazard sensing. On top of that, the system's emission preference towards the L-band region with the increase in EDF length, could be easily developed into a simplified L-band random laser. The inclination of the hybrid structure to support multiple resonant wavelengths could also be harnessed to advance the current multiwavelength random laser to high extinction ratio. Finally, it is important to gather experimental evidence in devising pertinent and practical applications, and the sustained chaotic regime is an intriguing phenomenon which opens discussion on potential spontaneous pulse burst emission exploitation.

## REFERENCES

- [1] H. Cao, "Review on latest developments in random lasers with coherent feedback," *J. Phys. A, Math. Gen.*, vol. 38, no. 2, p. 467, Dec. 2005.
- [2] H. Cao, J. Y. Xu, Y. Ling, A. L. Burin, E. W. Seeling, X. Liu, and R. P. H. Chang, "Random lasers with coherent feedback," *IEEE J. Sel. Topics Quantum Electron.*, vol. 9, no. 1, pp. 111–119, Jan. 2003.
- [3] V. Vuletic, "Lasers: Amplified by randomness," *Nat. Phys.*, vol. 9, no. 6, pp. 325–326, Jun. 2013.
- [4] D. S. Wiersma, "The physics and applications of random lasers," *Nature Phys.*, vol. 4, no. 5, pp. 359–367, May 2008.
- [5] D. S. Wiersma, "Laser physics: Random lasers explained?" *Nature Photon.*, vol. 3, no. 5, pp. 246–248, May 2009.
- [6] S. K. Turitsyn, S. A. Babin, A. E. El-Taher, P. Harper, D. V. Churkin, S. I. Kablukov, J. D. Ania-Castañón, V. Karalekas, and E. V. Podivilov, "Random distributed feedback fibre laser," *Nature Photon.*, vol. 4, no. 4, pp. 231–235, Feb. 2010.
- [7] S. K. Turitsyn, S. A. Babin, D. V. Churkin, I. D. Vatnik, M. Nikulin, and E. V. Podivilov, "Random distributed feedback fibre lasers," *Phys. Rep.*, vol. 542, no. 2, pp. 133–193, 2014.
- [8] Y. Li, P. Lu, X. Bao, and Z. Ou, "Random spaced index modulation for a narrow linewidth tunable fiber laser with low intensity noise," *Opt. Lett.*, vol. 39, no. 8, pp. 2294–2297, 2014.
- [9] W. L. Zhang, Y. Y. Zhu, Y. J. Rao, Z. N. Wang, X. H. Jia, and H. Wu, "Random fiber laser formed by mixing dispersion compensated fiber and single mode fiber," *Opt. Express*, vol. 21, no. 7, pp. 8544–8549, 2013.
- [10] Y. J. Rao, L. W. Zhang, J. M. Zhu, Z. X. Yang, Z. N. Wang, and X. H. Jia, "Hybrid lasing in an ultra-long ring fiber laser," *Opt. Express*, vol. 20, no. 20, pp. 22563–22568, 2012.
- [11] A. M. R. Pinto, M. Lopez-Amo, J. Kobelke, and K. Schuster, "Temperature Fiber laser sensor based on a hybrid cavity and a random mirror," *J. Lightw. Technol.*, vol. 30, no. 8, pp. 1168–1172, Apr. 15, 2012.
- [12] Y. Y. Zhu, W. L. Zhang, Y. J. Rao, Z. N. Wang, and X. H. Jia, "Output characterization of random fiber laser formed by dispersion compensated fiber," *IEEE Photon. Technol. Lett.*, vol. 26, no. 3, pp. 246–248, Feb. 1, 2014.
- [13] M. H. A. Bakar, F. R. M. Adikan, and M. A. Mahdi, "Rayleigh-based Raman fiber laser with passive erbium-doped fiber for secondary pumping effect in remote l-band erbium-doped fiber amplifier," *IEEE Photon. J.*, vol. 4, no. 3, pp. 1042–1050, Jun. 2012.
- [14] L. Wang, X. Dong, P. P. Shum, C. Huang, and H. Su, "Erbium-doped fiber laser with distributed Rayleigh output mirror," *Laser Phys.*, vol. 24, no. 11, 2014, Art. no. 115101.
- [15] L. Wang, X. Dong, P. P. Shum, and H. Su, "Tunable erbium-doped fiber laser based on random distributed feedback," *IEEE Photon. J.*, vol. 6, no. 5, Oct. 2014, Art. no. 1501705.
- [16] W. L. Zhang, S. W. Li, R. Ma, Y. J. Rao, Y. Y. Zhu, Z. N. Wang, X. H. Jia, and J. Li, "Random distributed feedback fiber laser based on combination of er-doped fiber and single-mode fiber," *IEEE J. Sel. Topics Quantum Electron.*, vol. 21, no. 1, Jan./Feb. 2015, Art. no. 0900406.
- [17] Y. Liu, X. Dong, M. Jiang, X. Yu, and P. Shum, "Multi-wavelength erbium-doped fiber laser based on random distributed feedback," *Appl. Phys. B, Lasers Opt.*, vol. 122, no. 9, p. 240, Sep. 2016.
- [18] C. Huang, X. Dong, S. Zhang, N. Zhang, and P. P. Shum, "Cascaded random fiber laser based on hybrid Brillouin-erbium fiber gains," *IEEE Photon. Technol. Lett.*, vol. 26, no. 13, pp. 1287–1290, Jul. 1, 2014.
- [19] I. A. Litago, R. A. Pérez-Herrera, M. Á. Quintela, M. López-Amo, and J. M. López-Higuera, "Tunable dual-wavelength random distributed feedback fiber laser with bidirectional pumping source," *J. Lightw. Technol.*, vol. 34, no. 17, pp. 4148–4153, Sep. 1, 2016.
- [20] V. DeMiguel-Soto, M. Bravo, and M. López-Amo, "Fully switchable multiwavelength fiber laser assisted by a random mirror," *Opt. Lett.*, vol. 39, no. 7, pp. 2020–2023, Apr. 2014.
- [21] N. H. Z. Abidin, M. H. A. Bakar, N. Tamchek, F. R. M. Adikan, and M. A. Mahdi, "Pump distribution effect in dual-wavelength Raman-erbium random distributed feedback fiber laser," *Opt. Express*, vol. 26, no. 12, pp. 15411–15419, Jun. 2018.
- [22] S. Sugavanam, M. Z. Zulkifli, and D. V. Churkin, "Multi-wavelength erbium/Raman gain based random distributed feedback fiber laser," *Laser Phys.*, vol. 26, no. 1, Jan. 2016, Art. no. 015101.
- [23] H. Wu, Z. Wang, W. Sun, Q. He, Z. Wei, and Y.-J. Rao, "1.5  $\mu\text{m}$  low threshold, high efficiency random fiber laser with hybrid Erbium–Raman gain," *J. Lightw. Technol.*, vol. 36, no. 4, pp. 844–849, Feb. 15, 2018.
- [24] S. A. Babin, A. E. El-Taher, P. Harper, E. V. Podivilov, and S. K. Turitsyn, "Broadly tunable high-power random fibre laser," *Proc. SPIE*, vol. 8237, Feb. 2012, Art. no. 82373E.
- [25] S. Sugavanam, Z. Yan, V. Kamynin, A. S. Kurkov, L. Zhang, and D. V. Churkin, "Multiwavelength generation in a random distributed feedback fiber laser using an all fiber Lyot filter," *Opt. Express*, vol. 22, no. 3, pp. 2839–2844, Feb. 2014.
- [26] S. Sugavanam, N. Tarasov, X. Shu, and D. V. Churkin, "Narrow-band generation in random distributed feedback fiber laser," *Opt. Express*, vol. 21, no. 14, pp. 16466–16472, Jul. 2013.
- [27] A. R. Sarmani, M. H. A. Bakar, F. R. M. Adikan, and M. A. Mahdi, "Laser parameter variations in a Rayleigh scattering-based Raman fiber laser with single fiber Bragg grating reflector," *IEEE Photon. J.*, vol. 4, no. 2, pp. 461–466, Apr. 2012.
- [28] I. Aporta, M. A. Quintela, H. S. G. Roufael, and J.-M. López-Higuera, "Stability study of ultra-long Random distributed feedback fiber laser based on Erbium fiber," in *Proc. Workshop Specialty Opt. Fibers Appl.*, 2015, Paper WT4A.18.
- [29] A. R. Sarmani, M. H. A. Bakar, A. A. A. Bakar, F. R. M. Adikan, and M. A. Mahdi, "Spectral variations of the output spectrum in a random distributed feedback Raman fiber laser," *Opt. Express*, vol. 19, no. 15, pp. 14152–14159, Jul. 2011.
- [30] Y. Tang and J. Xu, "A random Q-switched fiber laser," *Sci. Rep.*, vol. 5, Mar. 2015, Art. no. 9338.
- [31] M. Chernysheva, S. Sugavanam, and D. Churkin, "Pulse bursts generation at 10 GHz intra-burst repetition rate in Quasi-lossless mode-locked erbium-doped fibre laser," in *Proc. Conf. Lasers Electro-Opt. Eur. Eur. Quantum Electron. Conf. (CLEO/Europe-EQEC)*, Jun. 2017, p. 1.
- [32] A. Yeniay, J.-M. Delavaux, and J. Toulouse, "Spontaneous and stimulated Brillouin scattering gain spectra in optical fibers," *J. Lightw. Technol.*, vol. 20, no. 8, pp. 1425–1432, Aug. 2002.
- [33] A. A. Fotiadi, "Random lasers: An incoherent fibre laser," *Nature Photon.*, vol. 4, no. 4, pp. 204–205, 2010.
- [34] Z. Wang, H. Wu, M. Fan, L. Zhang, Y. Rao, W. Zhang, and X. Jia, "High power random fiber laser with short cavity length: Theoretical and experimental investigations," *IEEE J. Sel. Topics Quantum Electron.*, vol. 21, no. 1, Jan./Feb. 2015, Art. no. 0900506.
- [35] E. A. Zlobina, S. I. Kablukov, and S. A. Babin, "Linearly polarized random fiber laser with ultimate efficiency," *Opt. Lett.*, vol. 40, no. 17, pp. 4074–4077, Sep. 2015.



**N. H. ZAINOL ABIDIN** received the B.E. degree (Hons.) in electrical and electronics from Vanderbilt University, Nashville, USA, in 2012, and the Ph.D. degree in photonics engineering with Universiti Putra Malaysia, where she is currently a Senior Lecturer. She is an active Member of the IEEE Young Professionals Malaysia. Her research interests include ultrafast photonics, fiber lasers, and sensors.



**M. H. ABU BAKAR** received the Ph.D. degree in photonics and fiber optic systems engineering from Universiti Putra Malaysia, Serdang, Malaysia, in 2012, where he is currently an Associate Professor. His current research interests include optical communication devices and sensors. He is a Senior Member of IEEE and a member of The Optical Society.



**Y. MUSTAPHA KAMIL** received the bachelor's degree in biomedical sciences (Hons.) from Universiti Kebangsaan Malaysia, in 2012, and Ph.D. degree in biomedical engineering from the Universiti Putra Malaysia, in 2018. She is currently the CEO of Inlazer Dynamics Sdn Bhd, a start-up company that provides fiber optic-based laser solutions. Her research interests include bio-optical fiber sensors and biomedical applications.



**M. THAMER ALRESHEEDI** received the B.Sc. degree (Hons.) in electrical engineering from King Saud University, Riyadh, Saudi Arabia, in 2006, and the M.Sc. degree (Hons.) in communication engineering and the Ph.D. degree in electronic and electrical engineering from Leeds University, Leeds, U.K., in 2009 and 2014, respectively. He is currently an Assistant Professor with the Department of Electrical Engineering, King Saud University. He is the author of a number of published papers. His research interests include adaptive techniques for optical wireless (OW), optical fiber communications, optical networks, indoor OW networking, and visible light communications.



**AHMAD FAUZI ABAS** received the B.Eng. degree in telecommunications engineering from Universiti Malaya, Kuala Lumpur, the M.Sc. degree in communications and networks engineering from Universiti Putra Malaysia, in 2002, and the Dr.Ing. degree in optical fiber communications from the University of Paderborn, Germany, in 2006. He has authored or coauthored over 100 scientific articles. He is currently an Associate Professor with King Saud University, Riyadh, Saudi Arabia.



**M. A. MAHDI** received the B.Eng. degree from Universiti Kebangsaan Malaysia, and the M.Sc. and Ph.D. degrees from Universiti Malaya, in 1996, 1999, and 2002, respectively. He joined the Faculty of Engineering, Universiti Putra Malaysia, in 2003. Since 1996, he has been involved in photonics research specializing in optical amplifiers, lasers, and sensors. He has authored or coauthored over 270 journal papers and 200 conference papers. His research interests include optical communications, optical sensors, and nonlinear optics.

...